Forecasting of intelligent thermal performance in two types of solar air heater using artificial neural networks

Maryam Zamanian[1], Abbas Rohani[1*], Khosrow Jafarpur[2]

(1. *Department of Biosystems Engineering, Faculty of Agriculture, Ferdowsi University of Mashhad, Azadi Square, Mashhad, Razavi Khorasan Province, P.O.Box 9177948974, Islamic Republic of Iran;*

2. *School of Mechanical Engineering, Shiraz University, Shiraz, Fars Province, P.O.Box 7193616548, Islamic Republic of Iran*)

Abstract: Applying solar collectors is a popular tool to harness solar energy.   In this research, a flat plate solar air collector with two types of glass cover, including slatted and flat, was investigated under direct solar radiation.   The study was conducted to evaluate the capability of perceptron neural network for modeling and predicting the efficiency of heat collectors by input parameters, input fluid mass flow, inlet and outlet air temperature from collector, temperature of the absorber, its thickness and porosity, and also solar energy.   Values obtained from tests were compared with the predicted values of the neural network.   According to obtained coefficient of determination, for flat (0.98) and slatted (0.99) glass cover, it has been concluded that using artificial neural networks is an accurate method to predict the thermal performance of solar air collectors.

Keywords: artificial neural networks, flat-plate solar air collectors, thermal performance.

1   Introduction

Nowadays due to high energy consumption and diminishing of the supplying resources, it has been expanded to use sustainable energies effectively especially solar energy. Applying solar collectors is one of the most popular methods for harnessing of solar energy. Solar air collector is simple in construction and maintenance. Lack of corrosion in air path, no air leakage, absorber conductivity, non-icing fluid are among the advantages of solar air collector to the liquid-type ones. The main problem of these collectors is low thermal efficiency that is because of the low heat transfer coefficient between the absorber and the air (Mohamad, 1997). So far, two types of absorber have been used in solar air collectors' porous absorber and nonporous one. The main disadvantage of nonporous absorber is

diminution of complete heat transfer between absorber and fluid that leads to the low thermal efficiency because the convective heat transfer coefficient between air and the absorber plate is quite low; therefore, the temperature of the absorber plate would be high and radiation loss is quite large. These absorber plates are suitable for natural or private flow collectors, as it provides a low pressure drop and does not prevent the fluid moving (Duffie and Beckman, 1991).

In porous type, absorbing of the solar radiant heat and the heat convection between air and the absorber can effectively strengthen the air that passes through the collector absorber. It improves the quality of heat transfer coefficient and thermal efficiency. Also due to the cool air on the absorber plate, air passing losses from convection and radiation under a suction reduce heat (Fechner and Bucek, 1998).

Porous absorber plates have been studied in different studies such as absorber made of aluminum foil cut (Chiou et al., 1965), wire nets (Beckman, 1968; Hamid and Beckman, 1971), retail glass (Collier, 1979), pages made of black synthetic fiber (Bansal et al., 1983), and

[1] **Corresponding Author**: **Abbas Rohani**, Department of Biosystems Engineering, Faculty of Agriculture, Ferdowsi University of Mashhad, Iran. Tel: 05138805000. Email: arohani@um.ac.ir.

thick black cotton fabric (Zomorodian et al., 2001). Due to absorption and penetration depth of solar radiation the benefit of porous absorber is attributed to the lower thermal energy dissipation to environment (Duffie and Beckman, 1991).

Whilier (1964), studying solar air collector, found that the use of a transparent coating layer is necessary to increase the economic efficiency of the collector.

In a study conducted by Zomorodian et al. (2001), a thick black cotton fabric absorber and slatted glass cover with vertical distance between the slatted glass sheets (transpired cover) for 3, 5, 7 and 9 mm were used to reduce heat loss from the upper part of collector and to increase the thermal efficiency.

Sotudeh (2002) studied the effect of wind direction on thermal performance; it was shown that the thermal efficiency raised when the wind was perpendicular to the direction of grooves and the lowest one occurred when the wind was blowing along the grooves. The effect of the wind direction change was about 10 to 20 percent on thermal efficiency.

In another research, the FLUENT software was used to evaluate the numerical grid plates with heat transfer in parallel flow to the suction, and it was determined that thermal performance was dependent on the six dimensionless parameters. One of these dimension groups was $x = t/D$, the ratio of thickness to hole diameter. Increasing of the parameter raised the heat transfer surface area within the hole thus more heat transfer into the absorbing plate and resulted an increase in the thermal efficiency of the absorber (Razavikhosroshahi, 2003).

In a research by Zomorodian and Barati (2010), three perforated aluminum sheets were used with different porosities and thickness of 1.25 mm to enhance the heat transfer coefficient between the absorber and the air. To reduce heat losses from the upper surface, we used one layer of plain glass sheet cover. The results of the study introduced two better porosities (0.0177) & (0.0314) of absorber sheets for better thermal efficiencies under different operating conditions.

An artificial neural network (ANN) was trained to predict the useful energy extracted from domestic thermosyphon solar water heating systems and raise the temperature of stored water. The results showed that proper training of a neural network could be used to predict the performance of these systems under any weather conditions (Kalogirou et al., 1999a).

Two types of air solar collector with two different absorbers were used to forecast the complex nonlinear relationship between thermal performance and input parameters. The comparison between the predicted values and test data inferred that Levenberg-Marquardt (LM) model has the ability to understand the relationship between inputs and outputs. Also, the statistical error analysis suggested that LM model with three neurons in the hidden layer is optimal because the maximum coefficient of determination 0.9971 & 0.9985 and minimum root mean squared error (RMSE) 0.0418 & 0.0262 for two types of collectors was obtained that is satisfactory (Benli, 2013).

Sharma et al. (2012) had an overview about the application of artificial intelligence techniques in solar energy systems. For example, the use of ANN to predict the global solar radiation in the areas where direct measurement was not applicable (Alawi and Hinai, 1998). They predict on a daily basis the useful energy inferred from a complete solar system (Qout) and the temperature rise of the water in the storage tank (Tdmax) (Kalogirou et al., 1999b). Furthermore, they have used long term performance anticipation of domestic hot water systems with good precision (Kalogirou and Panteliou, 2000).

In other applications, the building was evaluated through simulation by ANN and it was combining with genetic algorithm to optimize thermal comfort and energy consumption in residential buildings (Magnier and Haghighat, 2010). And we used fuzzy logic to control the rolling drive performance as a regulator to ensure and guarantee the expected intensity to develop and design a fuzzy controller to control the rolling position with respect to solar radiation available (Lah et al., 2006), which are instances of ANN solar systems application in the study. In summary, ANN has been becoming increasingly popular in thermal engineering applications recently. Some studies have been reported about using ANN in thermal applications (Kalogirou, 2006; Mellita and Kalogirou, 2008; Sözen et al., 2005; Yang et al., 2003).

As a result, it can be said that artificial intelligence

techniques are suitable for significant improvements in efficiency and they predict the optimal set of operating parameters for solar energy systems. In these systems, there are many areas for using a combination of these methods with other optimization techniques to improve system performance. In addition, solar energy systems are used to save the Life Cycle (LCS) and Life Cycle Assessment (LCA). After running this way and training, the ANN model is capable of predicting satisfactory results for unknown data.

The objectives of the research are designing, building and evaluating a solar collector with porous absorber, slatted and flat glass cover and the effect of glass cover type and input parameters (input fluid mass flow, inlet and outlet air temperature from collector, temperature of the absorber, thickness and porosity of it and also solar energy) on thermal efficiency of the collector, and also the investigation of the efficiency by using the neural network models.

2   Materials and methods

In this study, two types of transpired solar air collector were tested and the effect of design parameters on the thermal efficiency was evaluated by the neural network. The tests were conducted in three replications on very clear sky days during 11 to 13 o'clock (average solar energy was reported to be 1040 W m^{-2} during the interval).

2.1   The solar air collectors

Collectors were evaluated with ANN in this study, shown in Figures 1 and 2 (Zomorodian and Barati, 2010), and as it is evident from figures, two porosity, σ_1= 0.0314 & σ_2=0.0177, was considered for porous aluminum absorber sheets to be considered as the effect of porosity on output, also dimensions of 110×75 and thickness of 2.5 mm for absorber sheets was considered (2 mm pore diameter and 1 cm distance, σ_1= 0.0314, and the other with 3mm diameter and 2 cm distance, σ_2=0.0177, has been used). The arrangement of poles on both sides was in square shape. In Figure 1, each page's porosity is obtained from the following equation (Arulanandam, 1995).

$$\sigma = \frac{A_{hole}}{A_{plate}} = \frac{\pi D^2}{4P^2} \qquad (1)$$

where, D is hole diameter (m) and P is holes iteration step.

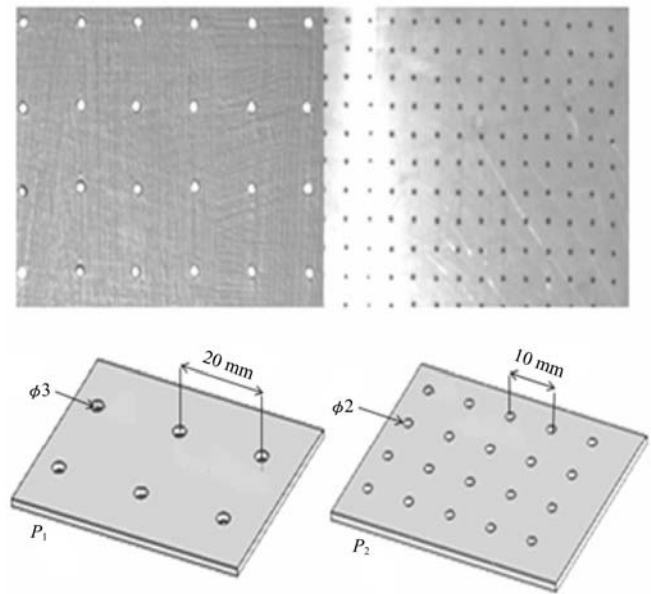Figure 1   Absorber plates and their porosities

2.1.1   Characteristics of measuring systems

Smart temperature sensors (SMT-160 ±0.5°C) were used for measuring of the temperature in different locations of the absorber, inlet and exhaust air.

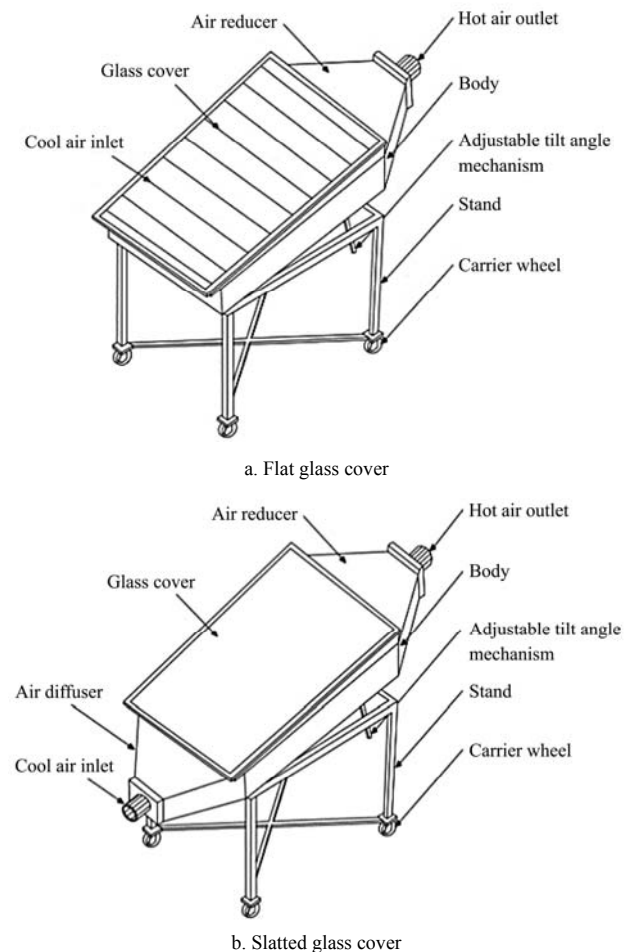

a. Flat glass cover

b. Slatted glass cover

Figure 2   An overview sketch of the solar collector

The air flow velocity which is one of the important parameters to calculate the thermal efficiency of the solar collector, was measured using an anemometer (Lutron (YK-2001A), Taiwan). The air flow velocity was converted to air flow rate by the following equation:

$$\dot{m} = \left(\frac{kg}{m^2 \cdot s}\right) = V\left(\frac{m}{s}\right) * A_1(m^2) * \rho\left(\frac{kg}{m^3}\right) / A_2(m^2) \quad (2)$$

where, $\dot{m}$ is air mass flux per unit area of collector (kg s^{-1} m^{-2}); V is inlet air speed (m s^{-1}); A_1 is air crossing area at the location of the anemometer (m^2); A_2 is evaluated surface of absorber (m^2) and ρ is air Inlet density (kg m^{-3}).

A constant speed centrifugal fan (Parma, 50 Hz, 1400 rpm, Italy) was used as an air flow source connected to an inverter (N50-015SF, 1.5 KW, Korea) to change the air flow rate. Besides, a silicon type pyranometer (Cassela, 0-2000 ±1W, UK) was used to measure solar radiation intensity.

2.1.2 Experimental procedure

The test rig was located on Faculty of Agriculture at Shiraz University. The inclination of collector and pyranometer by considering Equation (3) and according to 30-degree latitude of Shiraz, was set on 45 degrees towards the south (Duffie and Beckman, 1991),

$$\alpha = local\ altitude + 15 \quad (3)$$

To calculate the thermal efficiency of collector, Equation (4) was applied (Biondi et al., 1988),

$$EF = \dot{m}C_p \frac{(T_0 - T_i)}{G_T} \quad (4)\#$$

where, $\dot{m}$ is air mass flux per unit area of collector (kg s^{-1} m^{-2}); C_p is air specific heat capacity (J kg^{-1} °C^{-1}), T_0 is outlet air temperature (°C); T_i is inlet air temperature (°C) and G_T is the radiation flux on the collector (W m^{-2}).

2.2　ANN: a smart model

The main preference of ANN compared to other specialist systems is its speed, easiness and ability of modeling a multivariable problem to solve complex relationships between the variables and can elicit the nonlinear relationships through training data (Mellita and Kalogirou, 2008).

The data were divided randomly into three categories, 80% were given as training set, 10% as validation set and 10% as test Set (all data for a collector is 72). To control the number of training iterations and prevent overtraining problem, we used the validation dataset. In addition, we randomly choose 10% of the whole data set as the validation dataset. The training continued until the error of the validation dataset reached the minimum and the validation error failed to decrease for 5 iterations.

For modeling, the Multilayer Perceptron Neural Network (MLP) was used; this type of neural network produces output vector via the input vector, as showed Figure 3. The aim was adopting the correct parameters for the network to achieve real output close to their corresponding output as much as possible (Vakil-Baghmisheh, 2002). In network training, we have employed Backpropagation (BP) algorithm and Levenberg-Marquardt (LM) method. Furthermore, to implementing the ANN models, a computer code was developed in MATLAB software. To find the optimal weights between neurons, the LM training algorithm was used. The weights were updated using the Equation 5.

$$w_{ij}(n+1) = w_{ij}(n) - \eta \times \frac{\partial E}{\partial w_{ij}} + \alpha(w_{ij}(n) - w_{ij}(n-1)) \quad (5)$$

where, η is the learning rate adjusted between 0 and 1; α is the momentum factor at interval [0, 1]; w_{ij} is the connection weight between nodes i and j, also n is the number of iterations.

To evaluate the performance of a model some criteria have been defined in the literature. Among of them, root mean squared error (RMSE), mean absolute percentage error (MAPE) and coefficient of determination (R^2) (Rohani et al., 2011) (The coefficient of determination of the linear regression line between the predicted values from the neural network model and the actual output) are the most widely used performance evaluation criteria and may be used to compare the predicted and actual values which will be used in this study. They are defined as follows:

$$RMSE = \sqrt{\frac{\sum_{j=1}^{n}\sum_{i=1}^{m}(d_{ji} - p_{ji})^2}{nm}} \quad (6)$$

$$MAPE = \frac{1}{mn}\sum_{j=1}^{n}\sum_{i=1}^{m}\left|\frac{d_{ji} - p_{ji}}{d_{ji}}\right| \times 100 \quad (7)$$

$$R^2 = \frac{(\sum_{j=1}^{n}(dj - \bar{d})(pj - \bar{p}))^2}{\sum_{j=1}^{n}(d_j - \bar{d})^2 \cdot \sum_{j=1}^{n}(p_j - \bar{p})^2} \quad (8)$$

where, d_{ji} is the ith component of the desired (actual) output for the jth pattern; p_{ji} is the ith component of the predicted (fitted) output produced by the network for the jth pattern; $\bar{d}$ and $\bar{p}$ are the average of the desired output and predicted output, respectively; n and m are the number of patterns and the number of variable outputs, respectively. A model with the smallest RMSE, MAPE and the largest R^2 is considered to be the best.
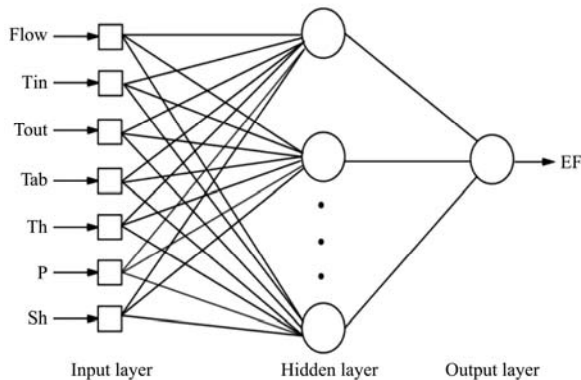

Figure 3   Configuration of the MLP

3   Results and discussion

To achieve the best ANN structure in order to evaluating the capability of perceptron neural network to modeling and predicting the efficiency of heat collectors by the input parameters, due to the constant number of inputs, the number of hidden layers (Haykin, 1999), we change the number of output neurons and each neuron activation functions and the number of neurons in the hidden layer. According to general approximation theorem, neural network with a hidden layer and with a sufficient number of neurons is able to approximate any optional continuous function (Haykin, 1999), so one hidden layer was selected for neural network. The number of hidden layer neurons has been obtained by using trial and error method. If there is not adequate number of neurons in the hidden layer, the network will not be able to learn well. Despite, this leads to weakening of the extended features of the network (Wang and Elhag, 2007). The results showed that the MLP neural network with 10 neurons in the hidden layer was able to learn the thermal performance over time (by foreseeing $\alpha = 0.9$, $\eta = 0.01$, epoch = 1000). To achieve better performance and accelerate the convergence of network, the momentum factor (α) was used (Gupta et al., 2003).

Because of the interaction between these two parameters on network performance, finding optimal values is difficult (Vakil-Baghmisheh and Pavešic, 2001). Besides, optimal values of the parameters were selected through trial and error method.

Considering the optimal number of neurons in the training phase, the results of the training data, validation step, trials stage and total, the best neural network models was determined for flat and slatted glass cover collectors.

3.1   ANN results statistical analysis

The prediction results of trained neural network based on input parameters has been shown in Table 1. The purpose of this stage is assessing generalizability features and merits of selected neural model. So, it was evaluated by using data other than the data collection of training model (a set of test data). According to the table, ANN has more desirable performance in the solar collector with slatted glass cover, because it has the maximum R^2 and minimum amount of standard error $RMSE$ and $MAPE$.

Table 1   Performance indicators of training, validation, and testing data for the best estimated models

Collector type	Criteria	Train	Validation	Test	Total[*]
Flat glass cover	R^2	0.999	0.9794	0.9407	0.9898
	RMSE	0.0058	0.0282	0.0513	0.019
	MAPE (%)	0.8779	5.7294	7.9981	2.0418
Slatted glass cover	R^2	0.9998	0.9907	0.9562	0.9914
	RMSE	0.0027	0.0228	0.0547	0.0186
	MAPE (%)	0.3413	3.89	4.6079	1.1011

Note: * training, validation and test data set.

Actual data and network forecast data were compared statistically. The results of the neural network model based on p-values in three phases: training, validation and test are given in Table 2. It can be said that in all cases P-value > 0.7, so it can be said that there is no significant difference between mean, variance and statistical distribution of experimental and predicted neural network data. These results show that we can trust on such networks because the generalizability of trained neural network is acceptable.

Also, according to R^2 for all three stages of network, it can be estimated the pattern of thermal performance variation by neural networks. In addition, according to the results we can say that collector with the slatted glass cover is more appropriate.

Table 2   Statistical comparisons between the actual and predicted values by the ANN

|		Test phase			Validation phase			Train phase		
		Distribution	Variance	Mean	Distribution	Variance	Mean	Distribution	Variance	
Flat cover	P	0.4232	0.6667	0.7701	0.9998	0.9642	0.93	0.9987	0.9728	Mean
	R^2			0.9407			0.9794			0.9814
Slatt cover	P	0.4232	0.5304	0.8743	0.8827	0.87	0.9886	0.9987	0.9546	0.999
	R^2			0.9562			0.9908			0.9998

Neural network convergence diagram to predict the thermal performance of slatted and flat glass cover collector is shown in Figure 4. RMSE becomes lower than 10 for the entire training, testing and validation set gradually by increasing the frequency and after 7 and 9 repeating for flat and slatted glass cover respectively, RMSE increases for validation data. Increasing in the number of algorithm iterations for training set reduces the amount of RMSE while after the seventh and ninth repeating will be useless but also increases the amount of RMSE in the validation set.

a. Flat cover

b. Slatted cover

Figure 4   Neural network convergence diagram to predict the thermal performance of flat and slatted cover collector. Mse: Root mean square error and Epochs: The number of iterations

Figure 5 shows R^2, as well as linear regression between the actual thermal performance of slat and flat glazing cover of solar air collector versus thermal performance predicted by the neural network. Based on these two criteria, best results are obtained when linear equation has lowest intercept and slope close to one (Output = 0.000, Efficiency = 1.000) between actual performance and the predicted one by the network in addition to high R^2. It is clear that R^2 between measured and predicted data in any case is very high ($R^2>0.9$). Also, the linear regressions between them have nearly the same slope close to one and relatively small intercept, so we can be sure to such networks. Assessing the ability of ANN techniques as an alternative method to predict the thermal performance of the solar air collector showed that ANN has high ability to provide reliable and accurate forecasts for thermal performance.
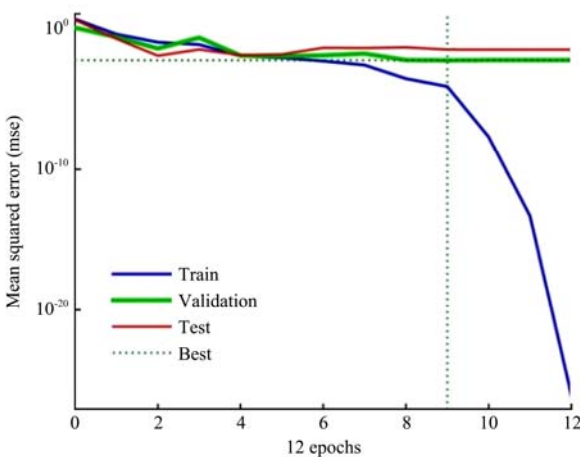
3.2   Collector performance

By using statistical analysis of the results of the impact of various parameters on the thermal efficiency of solar air collector, it can be said that inlet air flow, glazing, porosity and thickness parameters showed a very significant impact ($p=0.01$) on efficiency. By Figure 6, it can be said generally at low rates (mass flow rate less than 0.01 kg m^{-2} s^{-1}), for two charts with two different covers efficiency is almost equal which result in that at lower flow rates kind of cover does not have a significant effect on performance.

However, it was found from Figure 6 that at high flow rates, changes in minimum and maximum efficiency at collector with slatted cover is more than collector with flat cover. The reason can be stated as follows that on slatted type compared to flat one, on average, temperature difference between the air inlet and different parts of absorber is more. In other words, intake air of different parts of the slatted cover cools the absorber more uniformly. Also, at slatted glass cover, because the air
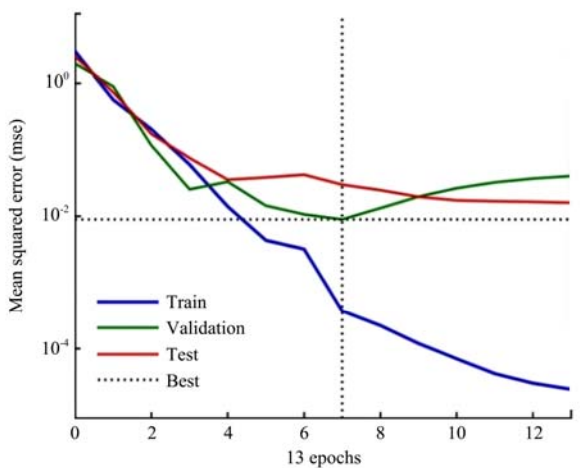
enters chamber from the gaps between glasses, hence it is cooled and absorbed heat by them is transferred. Therefore, compared with flat glass cover, it can be said

as absorber and glasses are cooler in slatted glass cover and consequently convective and radiative heat losses decreases thus higher efficiency is achieved.
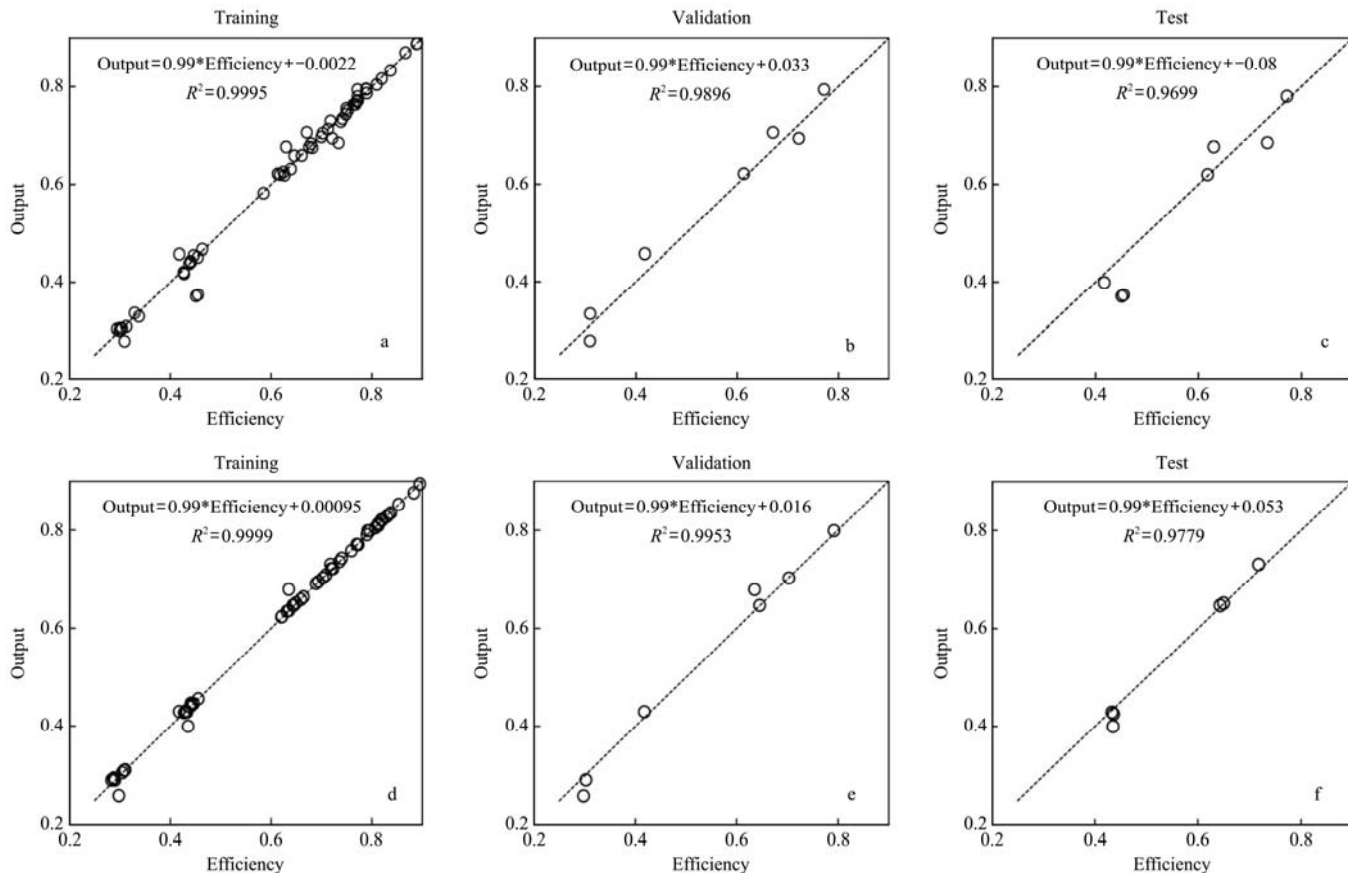

Figure 5   The relationship between actual performance and forecast values for collector for flat and slatted glass cover collector at the process of training, validation and test of network for training algorithm. Output: Predicted thermal performance by the network, Efficiency: Actual performance. (a-c) Flat glass cover, (d-f) Slatted glass cover
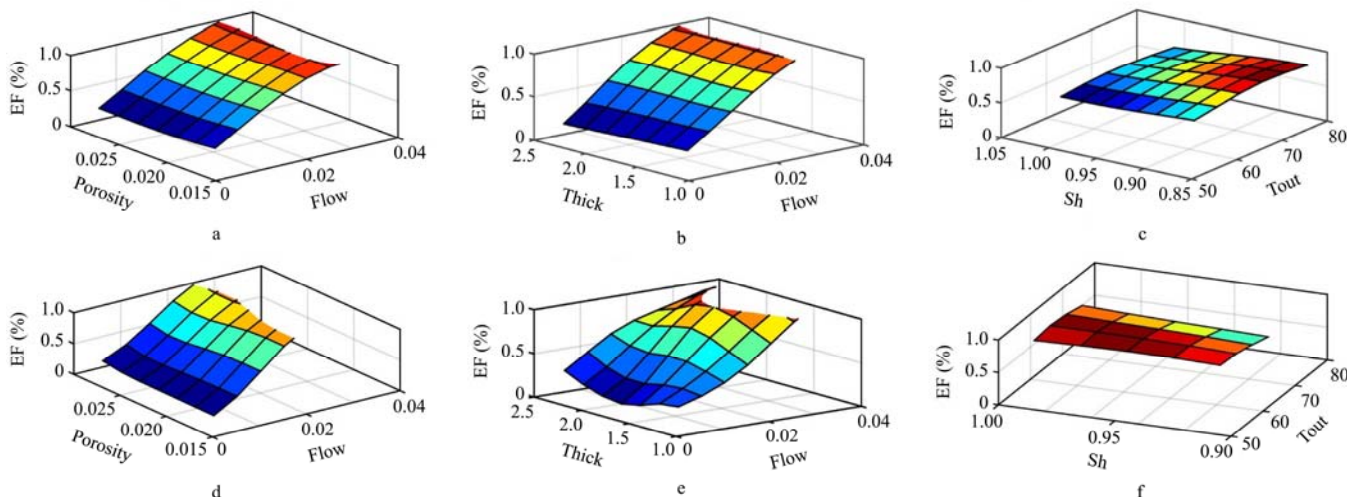

Figure 6   The effect of various parameters on the performance of solar air collector
(a-c) Flat glass cover collector (d-f) Slatted glass cover collector

Referring to Figure 6, it can be concluded that thermal efficiency increases by increasing the air flow rates due to greater contact volume of air flow rate which results in high rate of heat transfer coefficient and this reduces heat

losses by radiation and convection that results in increase in efficiency.

In addition, the diagram of Nusselt number compared to Reynolds has been determined in Figure 7. As we see

with increasing Reynolds number, Nusselt number for heat transfer fluid increases which showed an increase in convective heat transfer coefficient (h) by increasing the air mass flow rates as we reached the same conclusion.
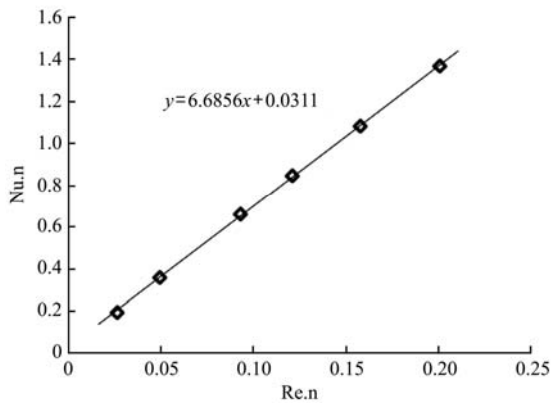

Figure 7   Changes in Nusselt number for Reynolds number

It is remarkable that variations of Nusselt number with Reynolds is linear (Incropera and Dewitt, 1996).

$$Re = \frac{VL}{\vartheta} \tag{8}$$

$$Nu = \frac{hL}{k} \tag{9}$$

Referring to the experimental results which indicate that absorber with lower porosity shows a better thermal efficiency at lower air mass flux. In fact, higher porosity and low flow cause the air to pass the lower part of the absorber and to rise the temperature of the parts near the exit of hot air. In other words, less porous absorber with the low flow rates have been the best heat transfer and minimal heat losses. This is because of the uniform passage of air from the absorber, but with increasing the air flow rate, air passing from the absorber become more uniform and porosity factor have been more effective. These differences agree with studies done by Zomorodian and Barati (2010). In other words, high efficiency of more porous absorber at high air flow rates can be caused by high porosity of this page that is due to more air contact with absorber. Moreover, maximum efficiency occurs when the thickness of the absorber plate is maximum. In fact, at maximum thickness, greater mass of material (aluminum) is heated by the sun (Razavikhosroshahi, 2003), or in other words while the air is crossing through the absorber, it covers more distance of pores and greater mass of absorber and cools the sheet. Accordingly, the exhaust air is warmer.

According to the results of charts, by increasing the temperature difference between the ambient and collector output air per unit of solar radiation, the thermal efficiency is reduced in both collectors that relevant to low air mass flow rate. In fact, by increasing the air mass flow rate, the temperature difference between the outlet air from the absorber compared to ambient air temperature decreased in all collectors which reduced the temperature difference between the exhaust air from the absorber and the environment per unit of solar radiation and increasing the thermal efficiency of the collector. According to the results, in general, it can be said that slatted glass cover collector has a higher performance.

4   Conclusions

Application of ANN to predict the relationship between the thermal performance of the solar air collector and two types of input variable was successful. The comparison between the predicted values and the values obtained from tests showed that this model was capable to predict the basic relationship between the input variables and the thermal performance of the collector. Also, statistical analysis of errors, showed reliability and accuracy of the model. R^2 of this model was obtained 0.98 for flat cover collector and 0.99 for slatted one which is desirable. Results indicate that the results predicted by the neural network and Backpropagation algorithm can accurately predict the performance of used solar air collector, which gives faster and simpler solutions to estimate the thermal performance of solar systems compared to limited laboratory methods.

As a result, we can say it is possible to train suitable neural network model for solar systems to be able to predict system performance under natural weather conditions.

References

Alawi, S. M., and H. A. Al-Hinai. 1998. An ANN-based approach for predicting global solar radiation in locations with no direct measurement instrumentation. *Renewable Energy,* 14(1-4): 199–204.

Arulanandam, S. J. 1995. A numerical investigation of unglazed transpired plate solar collectors under zero wind conditions. M. S. thesis. Ontario, Canada: Waterloo University.

Bansal, N. K., A. Bottcher and R. Uhleman. 1983. Performance of plastic solar air heating collector with a porous absorber. *Energy Research*, 7(4): 375–384.

Beckman, W. A. 1968. Radiation and convection heat transfer in a porous bed. *ASME Journal of Engineering for Power*, 90(1): 51–54.

Benli, H. 2013. Determination of thermal performance calculation of two different types solar air collectors with the use of artificial neural networks. *International Journal of Heat and Mass Transfer*, 60: 1–7.

Biondi, P., L. Cicala, and G. Farina. 1988. Performance analysis of solar air heater of conventional design. *Solar Energy*, 41(1): 101–107.

Chiou, J. P., M. M. El-Wakil, and J. A. Duffie. 1965. A slit-and-expanded aluminium foil matrix solar collector. *Solar Energy*, 9(2): 73–80.

Collier, R. K. 1979. The characterization of crushed glass as a transpired air heating solar collector material. In *Proc of the ISES Silver Jubilee Congress*, 264–268. Atlanta, GA., 27 May.

Duffie, J. A., and W. A. Beckman. 1991. *Solar Engineering of Thermal Processes*. 2nd ed. New York, USA: John Wiley & Sons.

Fechner, H., and O. Bucek. 1998. Investigations on several series produced collectors. *Renewable Energy*, 28: 293–302.

Gupta, M. M., L. Jin, and N. Homma. 2003. *Static and Dynamic Neural Networks*: *From Fundamentals to Advanced Theory*. Hoboken, New Jersey: John Wiley & Sons, Inc.

Hamid, Y. H., and W. A. Beckman. 1971. Performance of air-cooled radiatively heated screen matrices. *Journal of Engineering for Power*, 93(2): 221–224.

Haykin, S. 1999. *Neural Networks: A Comprehensive Foundation*. New York, USA: McMillan College Publishing Company.

Incropera, F. P., and D. P. Dewitt. 1996. *Fundamentals of Heat and Mass Transfer*. 4th ed. New York, USA: John Willey & Sons.

Kalogirou, S. A., S. Panteliou, and A. Dentsoras. 1999a. Artifcial neural networks used for the performance prediction of a thermosiphon solar water heater. *Renewable Energy*, 18(1): 87–99.

Kalogirou, S. A., S. Panteliou, and A. Dentsoras. 1999b. Modeling of solar domestic water heating systems using artificial neural networks. *Solar Energy*, 65(6): 335–342.

Kalogirou, S. A., and S. Panteliou. 2000. Thermosyphon solar domestic water heating systems long-term prediction using artificial neural networks. *Solar Energy*, 69(2): 163–174.

Kalogirou, S. A. 2006. Prediction of flat-plate collector performance parameters using artificial neural networks. *Solar Energy*, 80(3): 248–259.

Lah, M. T., B. Zupančič, J. Peternelj, and A. Krainer. 2006. Daylight illuminance control with fuzzy logic. *Solar Energy*, 80(3): 307–321.

Magnier, L., and F. Haghighat. 2010. Multiobjective optimization of building design using TRNSYS simulations, genetic algorithm, and Artificial Neural Network. *Building and Environment*, 45(3): 739–746.

Mellita, A., and S. A. Kalogirou. 2008. Artificial intelligence techniques for photovoltaic applications: a review. *Progress in Energy and Combustion Science*, 34(5): 574–632.

Mohamad, A. A. 1997. High efficiency solar air heater. *Solar Energy*, 60(2): 71–76.

Razavikhosroshahi, A. 2003. Numerical simulation study on heat transfer of porous absorber solar air collector with parallel airflow. M. S. diss. Shiraz, Iran: Shiraz University, Department of Mechanical Engineering.

Rohani, A., M. H. Abbaspour-Fard, and S. Abdolahpour. 2011. Prediction of tractor repair and maintenance costs using Artificial Neural Network. *Expert System Applications*, 38(7): 8999–9007.

Sharma, N., M. K. Chauhan, and R. Kumar. 2012. Applications of artificial neural network in solar thermal systems: a review. In *Proc. of the National Conference on Trends and Advances in Mechanical Engineering*, 188–194. Faridabad, Haryana, 19-20 October.

Sotudeh, A. 2002. Numerical 3-D simulation of airflow along heat transfer from porous absorber under suction with different angle. M. S. diss. Shiraz, Iran: Shiraz University, Department of Mechanical Engineering.

Sözen, A., E. Arcaklioğlu, and M. Özkaymak. 2005. Turkey's net energy consumption. *Applied Energy*, 81(2): 209–221.

Vakil-Baghmisheh, M. T., and N. Pavešić. 2001. Back-propagation with declining learning rate. In *Proc. of the 10th Electrotechnical and Computer Science Conference*, vol B, 297–300. Portorož, Slovenia, 11-13 September.

Vakil-Baghmisheh, M. T. 2002. Farsi character recognition using artificial neural networks. Ph.D. Diss. Ljubljana, Slovenia University of Ljubljana.

Wang Y., and T. M. S. Elhag. 2007. A comparison of neural network, evidential reasoning and multiple regression analysis in modeling bridge risks. *Expert Systems with Applications*, 32(2): 336–348.

Whillier, A. 1964. Performance of black-painted solar air heaters of conventional design. *Solar Energy*, 8(1): 31–37.

Yang, I. H., M. S. Yeo, and K. W. Kim. 2003. Application of artificial neural network to predict the optimal start time for heating system in building. *Energy Conversion and Management*, 44(17): 2791–2809

Zomorodian, A., J. L. Woods, and M. H. Raoufat. 2001. Performance characteristics of a transpired solar air heater. *Iran Agricultural Research*, 20(2): 139–154.

Zomorodian, A., and M. Barati. 2010. Efficient solar air heater with perforated absorber for crop drying. *Journal of Agricultural Science and Technology*, 12: 569–577.

Nomenclature:

A_{hole}	Surrounded level by every hole (cm^2)
A_{plate}	The total absorber surface (cm^2)
A_1	Air crossing area at the location of the anemometer (m^2)
A_2	evaluated surface of absorber (m^2)
D	Hole diameter (m)
EF	Thermal efficiency of collector (%)
H	Convective heat transfer coefficient (W m^{-2} K^{-1})
k	Conduction heat transfer coefficient (W m^{-1} K^{-1})
L	The characteristics of desired surface (m)
P	Holes iteration step
T_0	Outlet air temperature (°C)
T_i	Inlet air temperature (°C)
T_{max}	Collector stagnation temperature (°C)
V	Inlet air speed (m s^{-1})
σ	Absorber porosity (m^2/m^2)
$\dot{m}$	Air mass flux per unit area of collector (kg s^{-1} m^{-2})
ρ	Air Inlet density (kg m^{-3})
α	The tilt angle of collector and pyranometer (°)
ϑ	Kinematic viscosity of the fluid (m^2 s^{-1})
C_p	Air specific heat capacity (J kg^{-1} °C^{-1})
G_T	The radiation flux on the collector (W m^{-2})
d_{ji}	The ith component of the desired (actual) output for the jth pattern
p_{ji}	ith component of the predicted (fitted) output produced by the network for the jth pattern
$\bar{p}$ & $\bar{d}$	the average of the predicted output and desired output respectively
n & m	The number of patterns and the number of variable outputs respectively